

# The FRB-SGR Connection

J. I. Katz,<sup>1\*</sup>

<sup>1</sup>*Department of Physics and McDonnell Center for the Space Sciences, Washington University, St. Louis, Mo. 63130 USA*

17 November 2020

## ABSTRACT

The discovery that the Galactic SGR 1935+2154 emitted FRB 200428 simultaneous with a gamma-ray flare demonstrated the common source and association of these phenomena. If FRB radio emission is the result of coherent curvature radiation, the net charge of the radiating “bunches” or waves may be inferred from the radiated fields, independent of the mechanism by which the bunches are produced. A statistical argument indicates that the radiating bunches must have a Lorentz factor  $\gtrsim 10$ . The observed radiation frequencies indicate that their phase velocity (pattern speed) corresponds to Lorentz factors  $\gtrsim 100$ . Coulomb repulsion implies that the electrons making up these bunches have yet larger Lorentz factors, limited by their incoherent curvature radiation. These electrons also Compton scatter the soft gamma-rays of the SGR. In FRB 200428 the power they radiated coherently at radio frequencies exceeded that of Compton scattering, but in more luminous SGR outbursts Compton scattering dominates, precluding the acceleration of energetic electrons. This explains the absence of a FRB associated with the giant 27 December 2004 outburst of SGR 1806–20. SGR with luminosity  $\gtrsim 10^{42}$  ergs/s are predicted not to emit FRB, while those of lesser luminosity can do so. “Superbursts” like FRB 200428 are produced when narrowly collimated FRB are aligned with the line of sight; they are unusual, but not rare, and “cosmological” FRB may be superbursts.

**Key words:** radio continuum: transients, gamma-rays: general, stars: magnetars, stars: neutron

## 1 INTRODUCTION

Soft Gamma Repeaters (SGR) have long been candidates for the sources of Fast Radio Bursts (FRB). SGR are believed to originate in young neutron stars with extremely high magnetic fields and to be powered by dissipation of their magnetostatic energy (Katz 1982; Thompson & Duncan 1992, 1995), offering an ample source of energy. The energies  $\sim 10^{40}$  ergs of even “cosmological” FRB are a tiny fraction of the  $\sim 10^{47}$  ergs of magnetostatic energy of a neutron star with a  $\sim 10^{15}$  gauss field, a value inferred from the spindown rates of some SGR, measured in their quiescent Anomalous X-ray Pulsar (AXP) phases.

SGR also have short characteristic time scales. The most intense parts of their outbursts typically last  $\sim 0.1$  s, as did the outburst of SGR 1935+2154 simultaneous with FRB 200428. Upper bounds on the rise times of the three giant Galactic SGR outbursts were  $< 1$  ms (Katz 2016). Although the temporal structure of SGR have not been measured on the scale of the fastest temporal structure of FRB ( $\sim 10 \mu\text{s}$  (Cho *et al.* 2020)), the fact that both display extremely short time scales, shorter than any other astronomical time scale except those of pulsar pulses, suggests an association. This hypothesis has been advanced by many authors (Connor, Sievers & Pen 2016; Cordes & Wasserman 2016; Dai *et al.* 2016; Katz 2016; Zhang 2017; Wang *et al.* 2018; Wadiasingh & Timokhin 2019); see Katz (2018a) for a review.

The discovery of FRB 200428 in association with an outburst of SGR 1935+2154 demonstrated that FRB and SGR can be produced by the same events but raises four questions:

- (i) Why is SGR 1935+2154 different from other SGR, producing an observable FRB when the much more powerful 27 December 2004 giant eruption of SGR 1806–20 did not?
- (ii) What are the parameters of the emitters?
- (iii) Why do SGR 1935+2154 bursts range by  $\geq 8$  orders of magnitude in  $F_{radio}/F_{\gamma}$ ?
- (iv) What predictions can we make?

## 2 THE PROBLEM

FRB 200428, with fluence  $\sim 1.5 \times 10^6$  Jy-ms was discovered by CHIME/FRB (CHIME/FRB Collaboration 2020) and by STARE2 (Bochenek *et al.* 2020) during an outburst of the SGR 1935+2154<sup>1</sup> observed by INTEGRAL (Mereghetti *et al.* 2020), Insight-HXMT (Li *et al.* 2020), Konus-Wind (Ridnaia *et al.* 2020) and AGILE (Tavani *et al.* 2020) and consistent with the location of the SGR. A burst detected two days later by FAST (Zhang *et al.* 2020) had a fluence of  $\sim 60$  mJy-ms, a factor  $\sim 4 \times 10^{-8}$  times that of FRB 200428, while Kirsten *et al.* (2020) found two bursts of fluences  $\sim 112$  Jy-ms and  $\sim 24$  Jy-ms, about 1.4 s apart, 26 days after FRB 200428.

The ratio of the STARE2 (Bochenek *et al.* 2020) radio to

\* E-mail katz@wuphys.wustl.edu

<sup>1</sup> Sometimes referred to as J1935+2154.

the Insight-HXMT soft gamma-ray (Li *et al.* 2020) fluences of SGR 200428 was  $\sim 2 \times 10^{12}$  Jy-ms/(erg/cm<sup>2</sup>). This was several orders of magnitude greater than the upper limit of  $10^7$  Jy-ms/(erg/cm<sup>2</sup>) set by Tendulkar, Kaspi & Patel (2016) on any FRB associated with the giant 27 December 2004 outburst of SGR 1806–20.

The large observed radio-frequency fluence (Bochenek *et al.* 2020) of FRB 200428, taking a distance of 6 kpc, a compromise among the 12.5 kpc (Kothes *et al.* 2018), 9.1 kpc (Zhong *et al.* 2020) and 6.6 kpc (Zhou *et al.* 2020) estimated for the embedding SNR G57.2+0.8 and the 2–7 kpc estimated by Mereghetti *et al.* (2020) from dust-scattered SGR emission, implies an isotropic-equivalent emitted energy  $\sim 10^{-6}$  that of a nominal 1 Jy-ms “cosmological” FRB at  $z = 1$ . Any explanation of FRB as products of SGR must be consistent with “cosmological” FRB whose radio emission is several orders of magnitude more energetic than that of FRB 200428 and with the radio-to-gamma ray fluence ratio of FRB 200428 more than five orders of magnitude greater than that of SGR 1806–20. A number of theoretical interpretations have been suggested (Lu, Kumar & Zhang 2020; Lyutikov & Popov 2020; Margalit *et al.* 2020; Wang, Xu & Chen 2020; Wang 2020).

A past argument (Katz 2020) against a neutron star origin of FRB was the absence of periodicity in repeating FRB, particularly in the well-studied FRB 121102 (Zhang *et al.* 2018). SGR 1935+2154 has a period of 3.245 s (Israel *et al.* 2016), which would be expected to modulate the observable activity of FRB 200428, whatever its mechanism of emission, unless its magnetic field be a dipole aligned with the spin axis. The few extant detections of FRB 200428 are insufficient to test this prediction.

An additional argument (Katz 2020) was that the FRB sky was not dominated by Galactic FRB, and that therefore their sources must not be distributed with the stellar population whose inverse distance squared-weighted mass distribution and visible and other radiation are dominated by the Galactic disc. The 1.5 MJy-ms fluence of FRB 200428, about two orders of magnitude greater than the cumulative fluence of all other observed FRB, now invalidates that argument.

### 3 THE HOST

The characteristic spindown age of SGR 1935+2154 was measured over about 120 days in 2014 to be 3600 y (Israel *et al.* 2016), several times shorter than the estimated age of SNR G57.2+0.8 (Kothes *et al.* 2018; Zhou *et al.* 2020) in which it is embedded. These values of the SNR age were inferred from larger estimates of its distance; the smaller distance values of Mereghetti *et al.* (2020) and Zhou *et al.* (2020) would lead to much lower values of the SNR’s age and might resolve the disagreement.

Alternatively, the neutron star might now be in a period (at least several years long because the spindown was measured six years before the FRB) of unusual activity and unusually rapid spindown. Yet other alternatives include misidentification of the SGR with the SNR or the emergence of strong magnetic fields long after the neutron star’s birth (Biniamini *et al.* 2019).

## 4 CURVATURE RADIATION

FRB emission by a strongly magnetized neutron star has been explained as coherent curvature radiation (Kumar, Lu & Bhattacharya 2017). Its spectrum is the product of the spectrum of radiation emitted by accelerated point charges and the spectrum of the spatial structure of the coherent charge density distribution (Katz 2018b). The spectrum emitted by an accelerated point charge is very smooth and broad, so the observed spectral structure must be attributed to the distribution of charge density. The frequency and spectrum of the emitted radiation is determined by the phase velocity (pattern speed) of the deviations from charge neutrality that radiate. This must be distinguished from the velocities of the individual charges that also radiate incoherently. Describing the phase velocity of the plasma wave that bunches the charge density by its corresponding Lorentz factor  $\gamma_w$ , its minimum value  $\gamma_{min}$  for observed curvature radiation of angular frequency  $\omega$

$$\gamma_{min} \approx \left( \frac{3\omega R}{c} \right)^{1/3}, \quad (1)$$

where  $R$  is the radius of curvature of the guiding magnetic field line.

We have no direct evidence that the observed radiation is near this peak of the spectral envelope of curvature radiation, but selection effects favor the detection of the brightest radiation and make that plausible. This is the same argument that justifies the assumption of particle-field equipartition in incoherent synchrotron sources: the most efficient radiators are the most detectable. Taking  $R \sim 10^6$  cm, the neutron star radius, because the available energy density decreases rapidly with increasing distance from the neutron star, leads to an estimate  $\gamma_{min} \approx 100$ , only weakly dependent on the uncertain parameters.

The observed, comparatively narrow but varying, spectral bands of FRB radiation imply that there are comparatively few charge “bunches” radiating at any one time. If there were  $\gg \omega/\Delta\omega \sim 10$  such bunches, where  $\Delta\omega$  is the width of an individual band, each would likely have a different peak frequency of radiation corresponding to a peak in the Fourier transform of the spatial distribution of charge. The total spectrum of radiation, a sum over many such peaks, would be smooth and broad, rather than being confined to a few narrower bands as observed.

### 4.1 Radiating Charges

We model this distribution of charge density as a single charge  $Q$ , the amplitude of the peak of that Fourier transform; an actual point charge  $Q$  would radiate a very broad and smooth spectrum, not seen. The frequency-integrated power received per unit solid angle  $\mathcal{F}$  (Rybicki & Lightman 1979)

$$\mathcal{F} = \frac{dP}{d\Omega} = \frac{4Q^2 a_{\perp}^2}{\pi c^3} \gamma_w^8 \frac{1 - 2\gamma_w^2 \theta^2 \cos 2\phi + \gamma_w^4 \theta^4}{(1 + \gamma_w^2 \theta^2)^6}, \quad (2)$$

where  $a_{\perp} \approx c^2/R$  is the magnitude of the acceleration perpendicular to the velocity (and magnetic field line),  $\theta$  is the angle between the direction of observation and the velocity vector and  $\phi$  is an azimuthal angle. The half-width at half power of the radiation pattern  $\theta_{1/2} \approx 0.35/\gamma_w$ . For  $\gamma_w \theta \gg 1$  the final factor varies  $\propto (\gamma_w \theta)^{-8}$ , cancelling the factor of  $\gamma_w^8$ ,

leading to a result independent of  $\gamma_w$  but  $\propto \theta^{-8}$ . Taking  $\gamma_w \theta \ll 1$  and Eq. 1, if  $\gamma_w = \gamma_{min}$

$$Q \approx 0.2 \frac{c^{5/6}}{R^{1/3} \omega^{4/3}} \sqrt{\frac{dP}{d\Omega}} \approx 5 \times 10^{-8} \sqrt{\frac{dP}{d\Omega}} \quad (3)$$

in Gaussian cgs units for L-band radiation.

If  $\gamma_w \gg \gamma_{min}$  then the spectral peak and most of the radiated power is at frequencies above the observed L-band. As a result of integrating

$$\int \frac{dP}{d\Omega d\omega} d\omega \propto \int_0^{\omega_{max}} \omega^{1/3} d\omega \propto \omega_{max}^{4/3} \propto \gamma_w^4 \quad (4)$$

up to  $\omega_{max} \sim c\gamma_w^3/(3R)$ , the inferred spectrally integrated  $dP/d\Omega$  is multiplied by  $(\gamma_w/\gamma_{min})^4$ . Here we have taken the familiar angle-averaged result (Rybicki & Lightman (1979) Eq. 6.32) because the radiating charge distribution is likely to be very oblate (Sec. 4.3) and may contain multiple incoherently adding ‘‘bunches’’, so that an observer receives a radiation from a distribution of emitters whose velocities are spread over an angular width  $\sim 1/\gamma$ . Then Eq. 2 is replaced by

$$\mathcal{F}_{obs} = \left. \frac{dP}{d\Omega} \right|_{obs} = \frac{4Q^2 a_{\perp}^2}{\pi c^3} \gamma_w^4 \gamma_{min}^4 \frac{1 - 2\gamma_w^2 \theta^2 \cos 2\phi + \gamma_w^4 \theta^4}{(1 + \gamma_w^2 \theta^2)^6}, \quad (5)$$

where  $(dP/d\Omega)|_{obs}$  is the measured power density at the observational frequency, henceforth 1400 MHz, corresponding (Eq. 1) to  $\gamma_{min}$ .

For FRB 200428 (Bochenek *et al.* 2020; CHIME/FRB Collaboration 2020), taking a bandwidth of 400 MHz, a distance of 6 kpc and emission lasting 3 ms, and for a nominal ‘‘cosmological’’ FRB with a flux density of 1 Jy at  $z = 1$

$$\left. \frac{dP}{d\Omega} \right|_{obs} \sim \begin{cases} 1 \times 10^{36} \text{ erg/sterad-s} & \text{FRB 200428} \\ 2 \times 10^{42} \text{ erg/sterad-s} & z = 1 \end{cases} \quad (6)$$

and

$$Q \sim \begin{cases} 5 \times 10^{10} \gamma_r^{-2} \text{ esu} = 15 \gamma_r^{-2} \text{ C} & \text{FRB 200428} \\ 8 \times 10^{13} \gamma_r^{-2} \text{ esu} = 3 \times 10^4 \gamma_r^{-2} \text{ C} & z = 1, \end{cases} \quad (7)$$

where  $\gamma_r \equiv \gamma_w/\gamma_{min} \approx \gamma_w/100 \geq 1$ . These are only the charges whose (collimated) radiation is directly observed. There may be additional charges (much larger in total absolute magnitude) radiating in other directions, either simultaneously with the observed FRB, or at other times, if the FRB is part of a wandering or intermittent beam (Katz 2017a).

## 4.2 Empirical Lower Limit on the Lorentz Factor

The upper limits set by Lin *et al.* (2020) on FRB emission during other soft gamma-ray flares of SGR 1935+2154 of  $\lesssim 10^{-8}$  of FRB 200428 statistically constrain the Lorentz factor  $\gamma_w$  of the emitting charges (or their wave or pattern speed) if the emission is produced by acceleration perpendicular to the velocity. This bound applies to synchrotron radiation as well as to curvature radiation.

For a relativistic particle of Lorentz factor  $\gamma$ , emission at angles  $\theta \gg 1/\gamma$  is  $\mathcal{O}(\gamma\theta)^{-8}$  times that for  $\theta \ll 1/\gamma$  (Eq. 2). Brightness selection effects make it likely that FRB 200428 was observed at an angle  $\theta \lesssim \theta_{1/2} \approx 0.35/\gamma$ . If other observed soft gamma-ray bursts of SGR 1935+2154 produced radio bursts intrinsically similar to FRB 200428 but beamed in

directions statistically uniformly but randomly distributed on the entire sky, then of  $N$  such bursts the closest to the observer was likely at an angle  $\theta \sim \sqrt{4/N}$ . Then

$$\gamma_w \gtrsim 0.35 \left( \frac{\mathcal{F}_{max}}{\mathcal{F}_{min}} \right)^{1/8} \sqrt{\frac{N}{4}} \approx 10, \quad (8)$$

where  $N = 29$  is the number of SGR outbursts observed by Lin *et al.* (2020) and  $\mathcal{F}_{max}/\mathcal{F}_{min} \sim 10^8$  is the ratio of the brightest FRB observed (FRB 200428) to the upper limits set on FRB emission by all the other SGR outbursts. The effective (half-width at half-power) beam width  $\theta_{1/2} \approx 0.35/\gamma_w \lesssim 2^\circ$ . Continuing observation, increasing  $N$ , will either increase the lower bound of Eq. 8 or find a distribution of observed FRB strengths from which their angular radiation pattern may be inferred.

Eq. 8 describes the radiation of a point charge or a collimated beam. If the radiators are not perfectly collimated the lower bound would be greater because the observed  $\mathcal{F}_{max}/\mathcal{F}_{min}$  would be less than that describing the radiation pattern of an individual point charge.

This result is only approximate because observations are made in a fixed frequency band, while Eq. 2 represents an integral over all frequencies. This could be allowed for were the charge density spectrum known (as it is for a point charge), in which case the only complication would be the known angle-dependence of the Doppler shift. A wave spectrum of charge density radiates at different frequencies in different directions, but that spectrum is not known.

This method cannot be applied to the numerous observed bursts of FRB 121102 because no corresponding gamma-ray activity is detected and the number  $N$  of undetected radio bursts is not known. Because of limits on the sensitivity of X- and gamma-ray detectors, it is likely to be feasible only for Galactic FRB. However, it is possible to relate the observed duty factor  $D$  of a repeating FRB to its intrinsic activity duty factor  $D_{activity}$  if the beam of half-width  $\approx 0.35/\gamma_w$  is isotropically and randomly distributed on the sky and it is assumed that the observer must be within the beam half-power width to observe a burst. Then

$$D \approx \frac{\pi(0.35/\gamma_w)^2}{4\pi} D_{activity} \approx 0.03 \frac{D_{activity}}{\gamma_w^2}. \quad (9)$$

Because  $D_{activity} \leq 1$ , this relation can be inverted to obtain the bound

$$\gamma_w \gtrsim \sqrt{\frac{0.03}{D}}. \quad (10)$$

For known repeating FRB this bound is typically  $\gamma_w \lesssim 100$ .

Subsequent to the submission of the original version of this paper, Younes *et al.* (2020) reported a number  $N \gg 29$  of outbursts of SGR 1935+2154 that were not accompanied by FRB outbursts, but with upper limits  $\mathcal{F}_{min}$  (Eq. 8) much greater than those of Lin *et al.* (2020). This is consistent with the extreme collimation of FRB emission implied by Eq. 2.

## 4.3 Particle Energies

The requirement that the electrostatic repulsion of the charge bunches not disrupt them sets a lower bound on the particle energy  $E_e$  and Lorentz factor  $\gamma_{part}$ ; an electron must have sufficient kinetic energy to overcome repulsion by the net bunch charge  $Q$ . Coherent emission requires that the charge bunch

extend over a length  $\lesssim \lambda = c/\omega = \lambda/2\pi$  in its direction of motion and radiation in order that fields from its leading and trailing edges, arriving at times separated by  $\lesssim \lambda/c$ , add coherently. The minimum electron energy is

$$E_e = \gamma_{part} m_e c^2 \gtrsim \frac{Qe}{\ell}, \quad (11)$$

where  $\ell$  is approximately the largest dimension of the charge cloud. If the cloud is roughly spherical  $\ell \sim \lambda$  (about 3 cm for L-band radiation)

$$E_e \geq \begin{cases} 5\gamma_r^{-2} \text{ TeV} & \text{FRB 200428} \\ 8\gamma_r^{-2} \text{ PeV} & z = 1. \end{cases} \quad (12)$$

If the charge density be spread over a width  $\ell \sim R/\gamma_{min} \sim 10^4$  cm transverse to its direction of motion and radiation (a very oblate shape), the maximum permitted by the condition that the fields add coherently,

$$E_e \geq \begin{cases} 2\gamma_r^{-2} \text{ GeV} & \text{FRB 200428} \\ 3\gamma_r^{-2} \text{ TeV} & z = 1. \end{cases} \quad (13)$$

These values are lower limits. For the brighter FRB such as FRB 190523 (Ravi *et al.* 2019) they are much greater than for the nominal 1 Jy FRB. This implies  $\gamma_r \gg 1$  in order that  $E_e$  not be impossibly large.

The fact that FRB spectral structure typically consists of bands of width  $\Delta\omega \sim 0.1\omega$  indicates that the radiating waves have a minimum of  $\sim 10$  periodically spaced charge peaks. Individual regions of unbalanced charge may have charges an order of magnitude less than indicated by Eq. 7, with a corresponding reduction in  $E_e$ . These regions radiate coherently so the effective  $Q$  is reduced in Eq. 11 but not in Eqs. 2 and 5. This and the uncertain factor  $\gamma_r$  may make it possible to reconcile the values of Eq. 13 with the maximum electron energy  $\sim 0.2$  TeV, above which incoherent curvature radiation is energetic enough to make pairs in the large magnetic field. However, the much greater values of Eq. 12 are probably excluded at cosmological distances.

If we set  $\gamma_w = \gamma_{part}$  (so the radiating charges are not a wave or pattern speed but are the actual particle speed) and use Eq. 5 to determine  $Q$  and Eq. 11 we find

$$\gamma_{part} = \left( \frac{e}{\ell m_e c^2} \right)^{1/3} \left( \frac{\pi R^2}{4c} \frac{dP}{d\Omega} \Big|_{obs} \right)^{1/6} \gamma_{min}^{-2/3}. \quad (14)$$

Numerically

$$\gamma_{part} \sim \begin{cases} 300(10^4 \text{ cm}/\ell)^{1/3} & \text{FRB 20048} \\ 3500(10^4 \text{ cm}/\ell)^{1/3} & z = 1. \end{cases} \quad (15)$$

The corresponding  $\gamma_r$  are  $\sim 3 \times (10^4 \text{ cm}/\ell)^{1/3}$  and  $\sim 35 \times (10^4 \text{ cm}/\ell)^{1/3}$ , respectively. The charges  $Q$  may be found from Eq. 7.

#### 4.4 Accelerating the Electrons

Can electrons be accelerated to the energies indicated Eqs. 12 and 13? We calculate the required electric fields  $E$  by equating the power radiated by an electron in curvature radiation to the power delivered by the electric field  $\approx eEc$ . There are at least two possible criteria:

(i) The power of the incoherent curvature radiation emitted by electrons with the energies given by Eq. 12 or 13,

$E$ (esu/cm <sup>2</sup> )	FRB 200428	$z = 1$
$\ell = \lambda$	$3 \times 10^6 \gamma_r^{-8}$	$2 \times 10^{19} \gamma_r^{-8}$
$\ell = R/\gamma_{min}$	$3 \times 10^{-8} \gamma_r^{-8}$	$2 \times 10^5 \gamma_r^{-8}$

$t$ (s)	FRB 200428	$z = 1$
$\ell = \lambda$	$2 \times 10^{-7} \gamma_r^7$	$5 \times 10^{-17} \gamma_r^7$
$\ell = R/\gamma_{min}$	$6 \times 10^3 \gamma_r^7$	$1 \times 10^{-6} \gamma_r^7$

**Table 1.** Minimum values of electric field (upper) (multiply by 300 to convert to V/cm) required to balance incoherent curvature radiation losses of electrons at the energies required to overcome Coulomb repulsion by radiating bunches and energy loss times (lower) if there is no accelerating field. There is an additional criterion, that the electrons can be accelerated to the required energy (Eq. 11) in a length  $\lesssim R$ , that sets a more stringent minimum of  $E \gtrsim 5$  esu/cm<sup>2</sup> (1500 V/cm) for FRB 200428 if  $\ell = R/\gamma_w$ .

the energies required for electrons to form bunches with the charges inferred from the observed radiation without being disrupted by electrostatic repulsion, must not exceed the power imparted by the accelerating electric field. Their Lorentz factors  $\gamma_{part}$  are generally much greater than  $\gamma_{min}$ . The power an electron radiates as incoherent curvature radiation (Rybicki & Lightman 1979)

$$P_{curve} = \frac{2}{3} \frac{e^2}{c^3} a_{\perp}^2 \gamma_{part}^4 \approx \frac{2}{3} \frac{e^2}{c^3} \frac{c^4}{R^2} \gamma_{part}^4. \quad (16)$$

For a “bunch” of charge  $Q$  the elementary charge  $e$  is replaced by  $Q$  and  $\gamma_{part}$  is replaced by  $\gamma_w$  if the “bunch” is a wave or pattern on an underlying particle distribution with different Lorentz factors. Equating  $P_{curve} = eEc$  (Kumar, Lu & Bhattacharya 2017),

$$E \gtrsim \frac{2}{3} \frac{e}{R^2} \gamma_{part}^4, \quad (17)$$

where  $\gamma_{part} = Qe/\ell m_e c^2$  (Eq. 11), is required. The resulting numerical values are shown in Table 1. Faraday’s Law limits the electric fields that can be created by induction to  $E \lesssim B$ , and vacuum breakdown (Heisenberg & Euler 1936; Schwinger 1951; Stebbins & Yoo 2015; Lu & Kumar 2019) limits it to  $E \lesssim 2 \times 10^{12}$  esu/cm<sup>2</sup>. The curvature radiation model can be excluded as an explanation of “cosmological” FRB if  $\ell \sim \lambda$  unless  $\gamma_r \gtrsim 10$ , but smaller values of  $\gamma_r$  are consistent with larger but possible values of  $\ell$ .

(ii) The electric field must replenish the coherently radiated energy after the charge bunch has formed. As shown in Sec. 4.6, the kinetic energies of the charge bunches are very small, and must be replenished throughout a burst. This criterion is obtained from Eq. 16, replacing  $e$  by  $Q$ , using  $\gamma_w = 100$  and the power delivered by the electric field  $\approx QEc$ :

$$E \gtrsim \frac{2}{3} \frac{Q}{R^2} \gamma_w^4. \quad (18)$$

The numerical results are shown in Table 2, and are independent of  $\ell$  because the relevant Lorentz factor  $\gamma_w$  is determined by the observed frequency, not  $\ell$ .

It may not be necessary that work done by the electric field continuously replenish the kinetic energy of the coherently radiating charge bunches (Table 2). Energetic particles may be

$E$ (esu/cm <sup>2</sup> )	FRB 200428	$z = 1$
All $\ell$	$3 \times 10^6$	$5 \times 10^9$

**Table 2.** Minimum values of electric field (multiply by 300 to convert to V/cm) required to overcome coherent curvature radiation losses during the radiation of a charge bunch. Because the relevant Lorentz factor is that of the coherent wave the results do not depend on the values of  $\ell$  or of  $\gamma_r$  that determine the minimum particle Lorentz factor.

a sufficient energy reservoir, intermittently producing charge bunches by plasma instability, but if electrons cannot be accelerated to sufficient energy to form the necessary charge bunches (as is the case for spherical bunches with  $\ell \sim \lambda$  and smaller  $\gamma_r$ ) then sufficient coherent curvature radiation cannot be emitted.

#### 4.5 Origin of Accelerating Electric Field

Currents in a neutron star magnetosphere flow along closed magnetic loops, anchored in the neutron star in analogy to Solar prominences, as in the “magentar” model of SGR. A plasma instability may introduce a region of large “anomalous” resistivity, much greater than the microscopic plasma resistivity, interrupting the current flow and replacing the conductive region with an effective capacitor. Charge builds up on the boundaries of the newly insulating region.

This is described as an  $LC$  circuit with inductance  $L \sim 4\pi r/c^2$  (in Gaussian units), where  $r$  is the radius of the current loop (that may be as large as the magnetospheric radius  $R$ ) and capacitance  $C \sim A/(4\pi a)$ , where  $A$  is the cross-section of the current loop (that may be as large as  $\sim R^2$  for a distributed current) and  $a$  is the width of the gap that becomes insulating. The charge on the surfaces of the gap

$$Q_{gap}(t) = Q_0 \sin \frac{t}{\sqrt{LC}} = \sqrt{LC} J_0 \sin \frac{t}{\sqrt{LC}}, \quad (19)$$

where  $t$  is the time since the insulating gap opened,  $J_0$  was the interrupted current, and  $Q_0 = \sqrt{LC} J_0$ . For a distributed current and a wide gap  $A \sim r^2$  and  $\sqrt{LC} \sim r/c\sqrt{r/a}$ . Then  $J_0 \sim \Delta B r c / 4\pi$ ,  $Q_0 \sim \Delta B r^2 \sqrt{r/a} / 4\pi$ , the voltage drop  $V \sim Q_0 / C \sim \Delta B \sqrt{r a}$  and the electric field  $E \sim V/a \sim \Delta B \sqrt{r/a}$ . When the current loop is interrupted the required change in  $B$  is  $\Delta B \sim V/\sqrt{r a} \sim E \sqrt{a/r}$ . The fields indicated in the Tables for  $\ell \sim R/\gamma_w$  can be provided by plausible values of  $\Delta B$ . The potential drop  $V \sim \Delta B \sqrt{r a}$  must be  $\geq E_e/e$ . Because the values of  $r$ ,  $a$  and  $\gamma_r$  (entering in Table 1) are very uncertain it is not possible to make numerical estimates. The charges may be accelerated until their incoherent or coherent radiative losses equal the power imparted by the electric field, so that their energy density does not accumulate.

The charges  $Q_{gap}(t)$  are much larger than the radiating charges inferred from Eq. 7, but are not moving relativistically and do not radiate significantly. Radiation will be emitted by the changing magnetic field. On dimensional grounds, the expression for the power radiated in the dipole approximation is roughly valid, where the dipole moment  $\Delta\mu \sim \Delta B r^3$ , varies on a characteristic time scale  $\sim 1/\omega \sim c/r$  and  $r$  is the radius or characteristic size of the loop:

$$P \sim \frac{(\Delta\mu)^2 \omega^4}{3c^3} \sim \frac{(\Delta B)^2 c^3}{3\omega^2}. \quad (20)$$

For the maximum plausible  $\Delta B \sim 10^{15}$  gauss and the observed FRB L-band frequency,  $P \sim 10^{41}$  ergs/s and would be unbeamed, in contradiction to the argument of Sec. 4.2 for FRB 200428. Such unbeamed power would be insufficient to power “cosmological” FRB. Hence the radiation of Eq. 20 is unlikely to be related to observed FRB.

The achievable value of  $E$  may be limited by breakdown creation of electron-positron pairs, either the Schwinger vacuum breakdown that occurs for  $E \gtrsim 2 \times 10^{12}$  esu/cm<sup>2</sup>, or the curvature radiation-driven pair production cascade breakdown believed to occur in pulsars. Even if breakdown occurs, it may not necessarily “short out” the electric field and accumulated charges because the region of breakdown may still be resistive as a result of plasma instability. If the current loop is wide ( $\ell \sim R/\gamma_w$ ),  $E$  may be large enough to accelerate the electrons to the energies necessary to overcome Coulomb repulsion. Each portion of the area  $A$  accumulates charge, limited independently by breakdown in the capacitive gap, so that it may be possible to produce the necessary thin sheet charge distribution.

Faraday’s law

$$\nabla \times \vec{E} = -\frac{1}{c} \frac{\partial \vec{B}}{\partial t} \quad (21)$$

implies

$$\frac{E}{\Delta x} \sim \frac{1}{c} \frac{\Delta B}{\Delta t}. \quad (22)$$

$\Delta B \leq B$  (defining  $B$  as its maximum magnitude). Causality requires  $\Delta t \geq \Delta x/c$  so that

$$E \lesssim \Delta B \leq B. \quad (23)$$

This is a general limit on the electric fields that can be produced in a relaxing current-carrying magnetosphere.

Changing the magnetic field within a loop of area  $r^2$  by  $\Delta B$  in a time  $\tau$  produces an inductive electromotive force (EMF)

$$\begin{aligned} V_{inductive} &\sim \frac{r^2 \Delta B}{c\tau} \\ &\sim 3 \times 10^{10} \frac{\Delta B}{10^8 \text{ gauss}} \frac{r^2}{10^{12} \text{ cm}^2} \frac{0.1 \text{ s}}{\tau} \text{ esu/cm} \end{aligned} \quad (24)$$

and an electron energy

$$\begin{aligned} E_e &= eV_{inductive} \\ &\sim 10 \frac{\Delta B}{10^8 \text{ gauss}} \frac{r^2}{10^{12} \text{ cm}^2} \frac{0.1 \text{ s}}{\tau} \text{ TeV}. \end{aligned} \quad (25)$$

In FRB 200428 the EMF required to accelerate particles to the minimum energy for  $\ell = \lambda$  and  $\gamma_r = 1$  (Eq. 12) can be provided by  $\Delta B \sim 10^8$  gauss if the loop encompasses much of the magnetosphere ( $R \sim 10^6$  cm) and if  $\tau \sim 0.1$  s, as observed for SGR. If  $\ell = R/\gamma_w$  and  $\gamma_r = 1$  (Eq. 13),  $\Delta B \sim 2 \times 10^4$  gauss would be sufficient. For a nominal 1 Jy-ms FRB at  $z = 1$ ,  $\ell \sim \lambda$  and  $\gamma_r = 1$  would require  $\Delta B \sim 10^{11}$  gauss but  $\ell \sim R/\gamma_w$  and  $\gamma_r = 1$  would only require  $\Delta B \sim 3 \times 10^7$  gauss. Without a detailed understanding of the magnetohydrodynamics and plasma physics of SGR activity we cannot decide if these values are plausible, but they violate no physical law.

#### 4.6 Energetics

The magnetic energy dissipated is obtained using Eq. 24 and  $r \sim R$  to obtain the minimum  $\Delta B$  required to accelerate

electrons to the energy  $E_e = V_{inductive}e$ :

$$\begin{aligned} \mathcal{E} &\sim \frac{1}{3}B\Delta BR^3 \sim \frac{Bc\tau RQ}{3\ell} \\ &\sim \begin{cases} 3 \times 10^{39} \text{ ergs} & \text{FRB 200428} \\ 3 \times 10^{43} \text{ ergs} & z = 1, \end{cases} \end{aligned} \quad (26)$$

where the numerical values assume  $\ell \sim \lambda$  (larger  $\ell$  would lead to lesser values),  $\gamma_r = 1$  and the observed width of FRB outbursts  $\tau \sim 0.1$  s; for FRB 200428  $B = 2 \times 10^{14}$  gauss (Israel *et al.* 2016) and for a burst at  $z = 1$   $B = 10^{15}$  gauss have been assumed. The value of  $\mathcal{E}$  for FRB 200428 is consistent with the observed X-ray fluences of SGR 1935+2154. For ‘‘cosmological’’ FRB the value of  $\mathcal{E}$  is consistent with giant outbursts of Galactic SGR, but the argument of Sec. 4.8 indicates that only less powerful SGR outbursts may produce FRB.

Eq. 12 ( $\ell = \lambda$ ) would permit  $\sim 10^6$  bursts in the lifetime of SGR 1934+2154 and  $\sim 10^4$  repetitions for the nominal ‘‘cosmological’’ FRB if  $B \sim 10^{15}$  gauss. The number of repetitions could be several thousand times greater if  $\ell = R/\gamma_w$  (Eq. 13). These values are obtained from the required inductive EMF, not directly from the change in magnetostatic energy. If the magnetic field is regenerated from internal motions, there could be yet more repetitions. Weaker ‘‘cosmological’’ bursts, such as those of FRB 121102, require smaller  $Q$ ,  $E_e$ ,  $V_{inductive}$ , and  $\Delta B$ , and could repeat many more times during the active lifetimes of their sources.

The electric fields within the charge bunches

$$\begin{aligned} E &\sim \frac{Q}{\ell^2} \\ &\sim \begin{cases} 5 \times 10^2 (R/100\ell)^2 \gamma_r^{-2} \text{ esu/cm}^2 & \text{FRB 200428} \\ 8 \times 10^5 (R/100\ell)^2 \gamma_r^{-2} \text{ esu/cm}^2 & z = 1. \end{cases} \end{aligned} \quad (27)$$

If  $\ell \sim \lambda$  and  $\gamma_r \sim 1$  the field estimated for the cosmological FRB exceeds the Schwinger pair-production vacuum breakdown field (Heisenberg & Euler 1936; Schwinger 1951; Stebbins & Yoo 2015) several-fold. This paradox is resolved if the charge distribution is oblate, with  $\ell \gg \lambda$ , or if  $\gamma_r \gg 1$ . It might seem unlikely that charge would be concentrated into thin sheets perpendicular to its direction of motion and the magnetic field lines, but there is a strong selection effect favoring the observation of such emitting geometry because for it the fields add coherently, making the radiation stronger and more observable.

The kinetic energies of the motion of the net charges  $Q$  (Eqs. 7, 11) are very small,  $\sim 8 \times 10^{20}$  ergs for FRB 200428 and  $\sim 2 \times 10^{27}$  ergs for the nominal FRB at  $z = 1$  even if  $\gamma_r = 1$ . The energy driving the FRB, derived from magnetostatic energy, may flow directly to the radiating charges via the electric fields of Sec. 4.5, continually replenishing the kinetic energies of the radiating charges. The radiating region need not be quasi-neutral.

#### 4.7 Curvature Radiation vs. Compton Scattering

The relativistic electrons emitting curvature radiation are moving in the soft gamma-ray radiation field of the SGR. It is necessary to compare the power they emit in curvature radiation to their energy loss by Compton scattering. If the latter were to dominate, then it would be difficult to accelerate a population of electrons to the energies necessary to emit

a FRB. It is only possible to estimate the lower bound resulting from Compton scattering by the electrons contributing to the emission of coherent (FRB) curvature radiation. The density of any quasi-neutral plasma is unknown, and its Compton scattering power cannot be estimated. Hence the following is only a demonstration that Compton scattering need not be a catastrophic energy loss.

The power the electrons lose to Compton scattering is

$$P_{Compt} \approx n_\gamma N_e \sigma_{KN} E_e c, \quad (28)$$

where

$$n_\gamma \sim \frac{L_{SGR}}{4\pi R^2 h\nu_\gamma c} \quad (29)$$

is the number density of soft gamma-rays,  $N_e = Q/e$  is the number of electrons in the charge bunch,  $\sigma_{KN} \approx \pi r_e^2 \ln(2h\nu_\gamma E_e/m_e^2 c^4)/(h\nu_\gamma E_e/m_e^2 c^4)$  is the Klein-Nishina cross-section ( $r_e = e^2/m_e c^2$  is the classical electron radius) and  $E_e$  is the electron energy. In this regime of highly relativistic electrons scattering soft gamma-rays, nearly the entire electron kinetic energy is lost to the photon in a single scattering.

For FRB 200428, using Eqs. 7, 11 and 29,  $L_{SGR} \sim 6 \times 10^{39}$  ergs/s (at 6 kpc distance),  $h\nu_\gamma \sim 50$  keV (Mereghetti *et al.* 2020) and  $\gamma_w = 100$ , Eqs. 16 and 28 yield

$$\begin{aligned} \frac{P_{curve}}{P_{Compt}} &\sim \frac{8}{3} \frac{Qc(h\nu_\gamma)^2 \gamma_w^4}{L_{SGR} e^3 \ln(2h\nu_\gamma E_e/m_e^2 c^4)} \\ &\sim 300 \frac{6 \times 10^{39} \text{ ergs/s}}{L_{SGR}}. \end{aligned} \quad (30)$$

This value is uncertain, but is consistent with the assumption that Compton scattering losses do not exceed the radiated power and therefore the validity of Eq. 18 as a condition on the electric field. The use in Eq. 28 of the lower bound Eq. 11 on  $E_e$  is balanced, except for the slowly varying logarithm, by the energy dependence of  $\sigma_{KN}$ .

Despite the intense soft gamma-ray radiation field, the quadratic dependence of the coherent  $P_{curve}$  on  $Q$  makes it possible for it to exceed  $P_{Compt}$  that is only proportional to one power of  $Q = N_e e$ . An additional factor of  $Q$  enters  $P_{Compt}$  through the minimum electron energy (Eq. 11), but this is nearly cancelled by the inverse energy dependence of the Klein-Nishina cross-section. The number of coherently radiating charges in the bunch or wave  $N_e = Q/e$  is  $\sim 10^{20}$  for FRB 200428 and  $\sim 10^{23}$  for the cosmological FRB. These enormous values and the quadratic dependence on  $Q$  (or  $N_e$ ) that makes the FRB bright enough to observe also make Compton losses comparatively unimportant.

#### 4.8 Why Not SGR 1806–20

The strongest argument against the SGR-AXP hypothesis was empirical: During an unrelated observation, the giant 27 December 2004 outburst of SGR 1806–20 was in a radio telescope sidelobe but no FRB was detected (Tendulkar, Kaspi & Patel 2016). Although the sidelobe had sensitivity about 70 dB less than that of the main beam, the fact that the SGR was  $\sim 3 \times 10^5$  times closer than a typical ‘‘cosmological’’ FRB, as well as the extraordinary brightness of the SGR, led to an upper limit on the ratio of the radio to soft gamma-ray fluences of  $< 10^7$  Jy-ms/(erg/cm<sup>2</sup>). This is more than five orders

of magnitude less than the observed fluence ratio  $> 2 \times 10^{12}$  Jy-ms/(erg/cm<sup>2</sup>) of FRB 200428/SGR 1935+2154.

There are at least three possible explanations.

(i) Compton energy loss (Eq. 30). The soft gamma-ray luminosity of SGR 1806–20 during its giant outburst (Palmer *et al.* 2005) was more than seven orders of magnitude greater than that of SGR 1935+2154 during FRB 200428; this was only partially offset by a value of  $h\nu_\gamma$  less than two orders of magnitude greater, leading to a ratio  $P_{curve}/P_{Compt} \sim 10^{-3}$  for a burst like FRB 200428. Emission of GHz curvature radiation by SGR 1806–20 was suppressed by Compton scattering energy losses of the required relativistic electrons.

At intensities greater than  $\sim 10^{29}$  ergs/cm<sup>2</sup>-s (luminosities  $\gtrsim 10^{42}$  ergs/s for an isotropically emitting neutron star) radiation and energetic particles thermalize to black-body equilibrium by processes that turn two incoming particles into three outgoing particles: radiative Compton scattering, three photon pair annihilation (Katz 1996) and photon splitting in a strong magnetic field. The result is an opaque equilibrium photon-pair plasma in which relativistic particles suffer runaway Compton and Coulomb scattering energy loss and radio radiation cannot propagate.

(ii) Observations of FRB 200428 (Lin *et al.* 2020) indicate that the observable FRB/SGR flux ratio may vary from burst to burst by at least eight orders of magnitude, plausibly because of beaming (Sec. 4.2).

(iii) FRB radiation, unlike SGR, may be narrowly collimated, as suggested by Eq. 2. This is discussed in Sec. 4.9.

#### 4.9 Distribution of FRB Fluxes

If the beams of particle “bunches” emitting FRB are randomly distributed in direction, then the distribution of FRB fluxes can be obtained from Eq. 2. Results are shown in Fig. 1. The logarithmic slope is about  $-1/4$ ; for the corresponding relation between frequency and fluence the logarithmic slope is about  $-1/3$  because the brighter bursts with larger Doppler factors are shorter.

The distribution of observed fluxes is given by the convolution of the distribution shown in the Figure with the unknown distribution of intrinsic burst strengths. Nonetheless, this is consistent with the fact that FRB 200428 was discovered in  $\sim 10^7$  s of on-source observing time (Bochenek *et al.* 2020; CHIME/FRB Collaboration 2020), while a burst of  $\sim 4 \times 10^{-8}$  of its intensity was discovered in a 62 minute observing run (Zhang *et al.* 2020),  $\sim 3 \times 10^{-4}$  that long. It is also consistent with the comparative frequency of strong (10–100 times the median) bursts from FRB 180916.J0158+65 (Marthi *et al.* 2020).

“Superbursts” like FRB 200428 are produced when a narrowly collimated beam is directed towards the observer (Katz 2017a). They are unusual, but not rare, as indicated by the low slope in Fig. 1, and represent most of the time-integrated FRB power. The mean FRB power emitted is several orders of magnitude less than the isotropic-equivalent power of a superburst, or of any observed burst, because of collimation. “Cosmological” FRB may be superbursts of emitters whose mean FRB power is much less than their isotropic-equivalent power. This is also implied by their low duty factor (Katz 2018a).

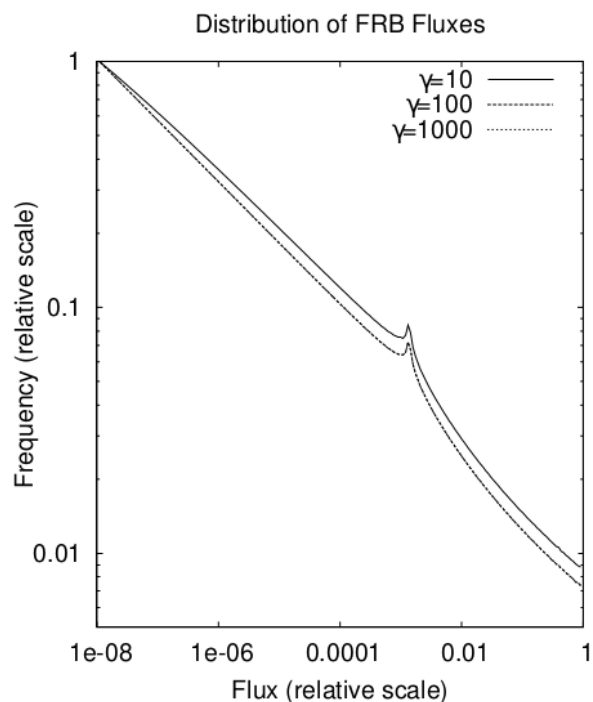


**Figure 1.** Frequency distribution of FRB fluxes emitted by randomly oriented, narrowly collimated, radiating charge “bunches”. The peak around  $\mathcal{F} \approx 10^{-3}$  arises because Eq. 2 is stationary around  $(\gamma\theta)^2 = 2$  and  $\cos 2\phi = 1$ . The distribution is almost independent of  $\gamma$  for  $\gamma \gg 1$  (the curves for  $\gamma = 100$  and  $\gamma = 1000$  are indistinguishable).

## 5 DISCUSSION

The discovery and identification of FRB 200428 resolved the first question about FRB: What astronomical objects produce them? It took 13 years from their discovery (and 7 years from the time their reality became generally accepted) to answer this question because of the difficulty of accurate localization. The similar difficulty of localizing gamma-ray bursts meant that their identification took 25 years, as did the recognition of extra-Galactic radio sources as the products of active galactic nuclei (AGN).

Identification of FRB with rotating neutron stars predicts that FRB activity should be modulated, at some level, at the rotation period. Periodicity has not been observed in FRB 121102, the only FRB for which abundant data exist (Zhang *et al.* 2018); see discussion in Katz (2019). If “cosmological” and Galactic FRB are qualitatively similar phenomena, periodicity should be detectable in any FRB that repeats frequently. Periodicity will be easier to detect in FRB identified with Galactic SGR because their periods would be known *a priori* from gamma-ray observations of the SGR/AXP.

The magnetospheric densities implied by Eq. 7 and the constraint on the dimensions of a radiating charge bunch  $< R/\gamma_w$  exceed the critical plasma density at observed FRB frequencies for the parameters of cosmological FRB. However, this limit on propagation is inapplicable. The plasma is strongly magnetized (so strongly that the electrons’ motion transverse to the field, the direction of the electric vector of a transverse wave propagating along the field, is quantized). In addition, the electrons’ longitudinal motion is highly rela-

tivistic (Eq. 11), increasing their effective mass by the factor  $\gamma_{part}$ . Finally, the radiating charge bunches may be confined to a shell thinner than the skin depth, like the currents in a metallic antenna radiating radio waves. Propagation and escape of the radiation are beyond the scope of this paper, but are issues that must be faced by any model in which FRB are emitted from a compact region, as required by their narrow temporal structure.

Identification of FRB with SGR does not itself explain their mechanism. Their high brightness temperatures require coherent emission, but there is no understanding of their charge bunching. Even in pulsars, discovered 53 years ago, the mechanism of charge bunching remains uncertain. Acceleration of relativistic particles is nearly ubiquitous in astrophysics (Katz 1991), and is also required to explain FRB, but is not understood from first principles; if we had not inferred it from observations in AGN, Solar activity, supernova remnants, pulsars, FRB and many other phenomena, we would not have predicted it.

The presence of an intense thermal (X-ray and soft gamma-ray) radiation field interferes with the acceleration and propagation of relativistic electrons. At sufficiently high radiation energy densities, radiative and particle energy thermalizes to a dense equilibrium pair-photon plasma (Katz 1996). This predicts that SGR with luminosities  $\gtrsim 10^{42}$  ergs/s do not make FRB comparable to FRB 200428.

The issues discussed here of the radiating charges  $Q$  and their implied electric fields extend beyond curvature radiation models, and apply however the charges are bunched, whether by plasma instability, maser amplification, or another mechanism. In any model, radiation can only be produced by accelerated charges or changing currents. It is difficult to produce beaming from changing currents because conservation of charge and the assumption of quasi-neutrality imply that current is constant along bundles of field lines; a relativistically moving current front cannot be produced without creating net charge density. The required  $Q$  are determined by the very general Eq. 7 and the particle Lorentz factors by Eq. 11 that are not specific to curvature radiation. This does not exclude sources outside an inner neutron star magnetosphere, but Eq. 2 applies and smaller  $Q$  imply larger  $\gamma_w$ , narrower beaming and, if  $\gamma_w$  is the Lorentz factor of an actual particle bunch, higher particle energy.

The extreme sensitivity of  $\mathcal{F}$  and  $\mathcal{F}_{obs}$  to  $\theta$  (Eqs. 2 and 5) may explain the excess (Katz 2017b) of very bright bursts; not enough bursts have been observed to sample fully the distribution of source strengths that otherwise would follow the  $d \ln N / d \ln \mathcal{F}_{obs} = -3/2$  distribution of sources homogeneously distributed in Euclidean space. This also suggests that repeating FRB may show “superbursts” exceeding their other observed bursts by orders of magnitude (Sec. 4.9). FRB 200428 was apparently such a superburst of SGR 1935+2154.

Younes *et al.* (2020) reported that the outburst of SGR 1935+2154 coincident with FRB 200428 had an X-ray spectrum distinct from that of its other outbursts, with a much higher energy cutoff. This is consistent with relativistic bremsstrahlung emitted by the FRB-emitting electrons, narrowly collimated towards the observer (parallel to the coherent radio frequency radiation), in addition to the roughly isotropic SGR radiation. Such relativistic bremsstrahlung would extend to photon energies  $E_e$  (Eq. 11), but its inten-

sity cannot be predicted from the radio intensity because they scale as different powers of  $Q$ .

Of the 30 SGR and AXP (the quiescent counterparts of SGR) and candidates now known (Olausen & Kaspi 2014), only SGR 1935+2154 has been detected as a source of FRB. What distinguishes SGR 1935+2154? Its spin period of 3.245 is near the short end of the distribution of spin periods, but it is not the shortest. Its inferred (from spindown, noting that SGR/AXP spindown rates vary by factors  $\mathcal{O}(1)$ ) surface magnetic field of  $2.2 \times 10^{14}$  gauss is well within the range of the fields of other SGR/AXP. I suggest that it is distinguished only by having a storm of activity during the short interval during which the wide field instruments CHIME/FRB and (especially) STARE2 have been operating. This explanation leads to the prediction that other SGR produce observable FRB during their storms of activity.

This prediction could be tested, and exploited if found to be correct, by staring at the positions of known SGR/AXP with small dedicated telescopes. The  $d = 4.5$  m diameter L-band telescopes in the DSA system (Kocz *et al.* 2019) would be suitable. Their ideal antenna gains ( $\approx \pi^2 d^2 / \lambda^2$ ) are about 38 dB, a great improvement in sensitivity over STARE2 that could not detect the FRB of SGR 1935+2154 other than its first, MJy-ms, giant burst. Staring gives a greater likelihood that a source will be within the field of view than CHIME/FRB (Amiri *et al.* 2018), whose instantaneous field of view is about 0.5% of the sky.

## ACKNOWLEDGEMENTS

I thank Wenbin Lu for many useful discussions and NSF AST 84-12895 for the HP 11C calculator used in this work.

## DATA AVAILABILITY

This is a theoretical paper that does not involve any new data.

## REFERENCES

- Amiri, M., Bandura, K., Berger, P. *et al.* 2018 ApJ 861, 48.  
 Biniamini, P., Hotokezaka, K., van der Horst, A. & Kouveliotou, C. 2019 MNRAS 487, 1426.  
 Bochenek, C., Kulkarni, S. Ravi, V. McKenna, D., Hallinan, G. & Belov, K. 2020 arXiv:2005.10828.  
 CHIME/FRB Collaboration 2020 arXiv:2005.10324.  
 Cho, H., Macquart, J. P. Shannon, R. M. *et al.* 2020 ApJ 891, L38 arXiv:2002.12539.  
 Connor, L., Sievers, J. & Pen, U.-L. 2016 MNRAS 458, L19.  
 Cordes, J. M. & Wasserman, I. 2016 MNRAS 457, 232.  
 Dai, Z. G., Wang, J. S., Wu, X. F. & Huang, Y. F. 2016 ApJ 829, 27.  
 Heisenberg, W. & Euler, H. 1936 Z. Phys. 98, 714.  
 Israel, G. L., Esposito, P., Rea, N. *et al.* 2016 MNRAS 457, 3448.  
 Katz, J. I. 1982 ApJ 260, 371.  
 Katz, J. I. 1991 ApJ 367, 407.  
 Katz, J. I. 1996 ApJ 463, 305.  
 Katz, J. I. 2016 ApJ 826, 226.  
 Katz, J. I. 2017a MNRAS 467, L96.  
 Katz, J. I. 2017b MNRAS 472, L85.  
 Katz, J. I. 2018a Prog. Part. Nucl. Phys. 103, 1.  
 Katz, J. I. 2018b MNRAS 481, 2946.



- Katz, J. I. 2019 MNRAS 487, 491.
- Katz, J. I. 2020 MNRAS 494, L64 arXiv:1912.00526.
- Kirsten, F., Snelders, M., Jenkins, M. *et al.* 2020 Nature 582, 351 arXiv:2007.05101.
- Kocz, J., Ravi, V., Catha, M. *et al.* 2019 MNRAS 489, 919.
- Kothes, R., Sun, X., Gaensler, B. & Reich, W. 2018 ApJ 852, 54.
- Kumar, P., Lu, W. & Bhattacharya, M. 2017 MNRAS 468, 2726.
- Li, C. K., Lin, L., Xiong, S.-L. *et al.* 2020 arXiv:2005.11071.
- Lin, L., Zhang, C. F., Wang, P. *et al.* 2020 arXiv:2005.11479.
- Lu, W. & Kumar, P. 2019 MNRAS 483, L93 arXiv:1810.11501.
- Lu, W., Kumar, P. & Zhang, B. 2020 MNRAS 498, 1397 arXiv:2005.06736.
- Lyutikov, M. & Popov, S. 2020 arXiv:2005.05093.
- Margalit, B., Beniamini, P., Sridhar, N. & Metzger, B. D. 2020 arXiv:2005.05283.
- Marthi, V. A., Gautam, T., Li, D. Z., Lin, H.-H., Main, R. A., Naidu, A., Pen, U.-L. & Wharton, R. S. 2020 MNRAS 499, L16 arXiv:2007.14404.
- Mereghetti, S., Savchenko, V., Gotz, D. *et al.* 2020 ApJ 898, L29 arXiv:2005.06335.
- Olausen, S. A. & Kaspi, V. M. 2014 ApJS 212, 6 <http://www.physics.mcgill.ca/~pulsar/magnetar/main.html>.
- Palmer, D. M., Barthelmy, S., Gehrels, N. *et al.* 2005 Nature 434, 1107.
- Ravi, V., Catha, M., D'Addario, L. *et al.* 2019 Nature 572, 352.
- Ridnaia, A., Svinikin, D., Fredericks, D. *et al.* 2020 arXiv:2005.11178.
- Rybicki, G. B. & Lightman, A. P. 1979 Radiative Processes in Astrophysics (Wiley, New York) Eqs. 4.92, 4.105, 6.32.
- Schwinger, J. 1951 Phys. Rev. 82, 664.
- Stebbins, A. & Yoo, H. 2015 arXiv:1505.06400.
- Tavani, M., Casentini, C., Ursi, A. *et al.* 2020 arXiv:2005.12164.
- Tendulkar, S. P., Kaspi, V. M. & Patel, C. 2016 ApJ 827, 1.
- Thompson, C. & Duncan, R. C. 1992 ApJ 392, L9.
- Thompson, C. & Duncan, R. C. 1995 MNRAS 275, 255.
- Wang, W., Luo, R., Yue, H. *et al.* 2018 ApJ 852, 140.
- Wadiasingh, Z. & Timokhin, A. 2019 ApJ 879, 4.
- Wang, J.-S. ApJ 900, 172 arXiv:2006.14503.
- Wang, W.-Y., Xu, R. & Chen, X. 2020 ApJ 899, 109 arXiv:2005.02100
- Younes, G., Baring, M. G., Kouveliotou, C. *et al.* 2020 arXiv:2006.11358.
- Zhang, B. 2017 ApJ 836, L32.
- Zhang, C. F., Jiang, J. C., Men, Y. P. *et al.* 2020 ATEL 13699.
- Zhang, Y. G., Gajjar, V., Foster, G. *et al.* 2018 ApJ 866, 149.
- Zhong, S. Q., Dai, Z. G., Zhang, H. M. & Deng, C. M. 2020 ApJ 898, L5 arXiv:2005.11109.
- Zhou, P., Zhou, X., Chen, Y., Wang, J.-S., Vink, J. & Wang, Y. 2020 arXiv:2005.03517.

This paper has been typeset from a  $\text{\TeX}/\text{\LaTeX}$  file prepared by the author.